

# Density inversion method for local basis sets without potential auxiliary functions: inverting densities from RDMFT

Sofia Bousiadi,<sup>1,2</sup> Nikitas I. Gidopoulos,<sup>3</sup> and Nektarios N. Lathiotakis<sup>1</sup>

<sup>1</sup>*Theoretical and Physical Chemistry Institute, National Hellenic Research Foundation, Vass. Constantinou 48, GR-11635 Athens, Greece*

<sup>2</sup>*Faculty of Physics, National and Kapodistrian University of Athens, Panepistimiopolis, Zografos, Athens 157 84, Greece*

<sup>3</sup>*Department of Physics, Durham University, South Road, Durham, DH1 3LE, United Kingdom*

(Dated: August 5, 2022)

A density inversion method is presented, to obtain the constrained, optimal, local potential that has a prescribed asymptotic behaviour and reproduces optimally any given ground-state electronic density. This work builds upon the method of [Callow *et al.* *J. Chem. Phys.*, 2020, **152**, 164114.] and differs in the expansion of the screening density in orbital basis element products instead of basis functions of an additional auxiliary set. We demonstrated the method by applying it to densities from DFT, Hartree-Fock, CAS-SCF and RDMFT calculations. For RDMFT, we demonstrate that density inversion offers a viable single-particle description by comparing the ionization potentials for atomic and molecular systems to the corresponding experimental values. Finally, we show that with the present method, accurate correlation potentials can be obtained from the inversion of accurate densities.

## I. INTRODUCTION

In Kohn-Sham (KS) DFT theory[1] a fictitious non-interacting system is constructed, whose density is equal to the density of the interacting one. The advantage of this construction is that the kinetic energy of the non interacting system is an explicit functional of the KS-orbitals. One main aspect of this theory is that the exchange and correlation term  $E_{xc}$  has to be approximated and the exchange and correlation potential in the single-particle KS equations is given by

$$v_{xc}[\rho](r) = \frac{\delta E_{xc}[\rho]}{\delta \rho(r)}. \quad (1)$$

So, in KS-DFT, the functional  $v_{xc}[\rho]$  is approximated and the density is calculated self-consistently. An interesting problem is the inverse KS problem, known also as the density inversion problem, that consists in finding the KS xc-potential  $v_{xc}(r)$  that corresponds to a prescribed electron density for a physical system. The uniqueness of such a potential is justified by the Hohenberg-Kohn theorem [2], which states that there is one to one density to potential mapping. It should be mentioned that, like the direct KS problem, the inverse one is also non-linear. This non-linearity stems from the fact that the density is the sum of the squares of the unknown orbitals. In practice, due to the use of finite basis sets the problem of inversion is not well posed and approximations and regularizations should be made.

Several methods have been developed for the inverse problem [3–13], which are of great importance, and many of which have been shown to be connected [14]. Some methods use as input orbitals, some wavefunctions, and others are density-based. It has also been proposed that Kohn-Sham potentials can be robustly constructed from the second order reduced density matrix[15–17]. It is a

challenge for DFT to embed accurate functionals. The potentials derived by inverting exact densities can aid in the development of new functionals by elucidating the weaknesses of approximate exchange and correlation potentials in reproducing important features[5, 6]. Additionally, inversion methods can also aid the improvement of existing functionals [18]. An interesting aspect of inversion methods is their connection with the optimised effective potential (OEP) problem[19]. As stated in Ref. [6] modification of the OEP method can lead to density to potential inversions. Generally, applications of inversion methods are numerous and are yet to be explored, they vary from analyzing errors of functionals to machine learning[20].

Recently, Callow et al[21] presented a method to solve the inverse problem in which the xc part of the inverted potential is constrained to decay at infinity as  $-\alpha/r$ , for a chosen value of  $\alpha$ . Although in principle any value (of order zero or one) can be chosen for  $\alpha$ , for the value  $\alpha = 1$ , the resulting potential has the expected asymptotic behavior of the exact KS potential. In that method, the variation quantity is the screening density  $\rho_{scr}$ , that is the effective density corresponding to the repulsive part of the KS potential (Hartree, exchange, and correlation) through Poisson’s equation. In this work, we present a variant of the inversion method of Callow et al.[21]. More specifically we avoid the expansion of the screening density in an auxiliary basis and instead, we adopt its expansion in products of the orbital basis elements, i.e. the same set used for the expansion of the electron density itself. In this way, the standard two-electron integrals are enough to calculate potential matrix elements. In addition, the corrections to the screening density in each iteration do not require projection on an auxiliary basis. Due to these differences, the present method is simpler since no auxiliary basis is required and no additional integrals of three basis functions need to be calculated.

We first applied the inversion method for densities obtained with DFT, Hartree-Fock, and CAS-SCF. Additionally, we applied it to densities obtained by minimizing functionals of the reduced density matrix functional theory (RDMFT) [22–34]. More specifically, we have applied the method to densities obtained from functionals such as BBC3[29], Power[30, 31], ML[28], and PNOF5[32]. In RDMFT [35], there is no default auxiliary single-particle system, like Kohn-Sham in DFT, e.g. for obtaining single particle spectrum. We show that a feasible single-particle scheme can be obtained via density inversion.

The present paper is organised as follows: In section II, we present the theory of our approach and the proposed algorithm. In Section III, we have included the results of applications by inverting LDA, HF, CAS-SCF, and RDMFT densities while in the last Section IV, concluding remarks have been included.

## II. THEORY

As in Ref. [21], the target is to find the optimal potential  $u$  that minimizes the Coulomb energy of the difference between the density,  $\rho_u$ , of a non interacting  $N$  electron system with potential  $u$  and the target density,  $\rho_t$ , that we want to invert,

$$U_C[u] = \frac{1}{2} \int d\mathbf{r} \int d\mathbf{r}' \frac{(\rho_u(\mathbf{r}) - \rho_t(\mathbf{r}))(\rho_u(\mathbf{r}') - \rho_t(\mathbf{r}'))}{|\mathbf{r} - \mathbf{r}'|}. \quad (2)$$

Minimization of this quantity was also considered in the derivation of the local Fock exchange (LFX) potential (obtained from the inversion of the HF density) in periodic systems [36], including metals [37]. The potential  $u$  in the above equation and through the whole discussion is the electron-electron repulsive part of the KS potential,  $u_{KS} = u_{en} + u$ , with  $u_{en}$  being the attractive nuclear potential. The single-particle Kohn-Sham (KS) equations that need to be solved are

$$\left[ -\frac{\nabla^2}{2} + u_{en}(r) + u(r) \right] \phi_i(r) = \epsilon_i \phi_i(r), \quad (3)$$

where  $u$  stands for the Hartree plus xc potential

$$u(r) = u_H(r) + u_{xc}(r). \quad (4)$$

The choice of minimization of  $U_C$  is based on the fact that, by doing so, the quantity

$$T_\Psi[u] = \langle \Psi | H_u | \Psi \rangle - E_u \quad (5)$$

is also minimized [38] over the effective potential  $u$ , and the minimizing potential  $u_s$  is the KS potential with density  $\rho_{u_s}$  equal to  $\rho_\Psi$ . By  $\Psi$  we denote the ground state wavefunction of the interacting system whose density is

the target density  $\rho_\Psi = \rho_t$ .  $H_u$  is a many-body (intermediate KS) Hamiltonian with an effective local potential  $u_{en} + u$  and density  $\rho_u$ . Finally,  $E_u$  is the sum of the  $N$  lowest eigenvalues of  $H_u$ .

Instead of  $u$ , a convenient variation quantity is the corresponding density  $\rho_{scr}$ , that we call screening density, associated to  $u$  through the relation

$$u(\mathbf{r}) = \int d\mathbf{r}' \frac{\rho_{scr}(\mathbf{r}')}{|\mathbf{r} - \mathbf{r}'|}. \quad (6)$$

As demonstrated in [21], if we correct the screening density in the direction of

$$\Delta\rho_{scr}(\mathbf{r}) = \epsilon \delta\rho(\mathbf{r}), \quad (7)$$

where  $\delta\rho = \rho_t - \rho_u$  and  $\epsilon$  is a small positive number, the objective function  $U_C$  of Eq. (2) will decrease. So the minimization can be performed in small consecutive steps along the  $\delta\rho$  direction, with  $\rho_u$  being updated in each step by solving the KS problem to obtain the KS orbitals. In this procedure, we need an initial guess  $\rho_{scr}^{(0)}$  which corresponds to a total screening charge  $Q_{scr}^{(0)} = \int d\mathbf{r} \rho_{scr}(\mathbf{r})$ . We note that, since  $\int d\mathbf{r} \Delta\rho_{scr}(\mathbf{r}) = 0$ , the screening charge remains constant,

$$Q_{scr}^{(i)} = Q_{scr}^{(0)}. \quad (8)$$

In Ref [39], we proposed that the quantity  $Q_{scr}$  is a measure for self interactions (SIs) and a necessary condition for a SI free method is that

$$Q_{scr} = N - 1, \quad (9)$$

where  $N$  is the number of electrons. Equivalently, one could only consider the exchange and correlation part of this quantity[40–43], that equals to -1. However, we choose to deal with the whole screening density in consistency with our previous work[44–47] Choosing  $\rho_{scr}^{(0)}$  to satisfy the above condition, the effective potential  $u^{(0)}(r)$  will have the correct asymptotic behavior  $(N - 1)/r$  of Hxc part of the exact KS potential. Thus, with the present inversion method, we find the optimal  $u(r)$  that minimizes the objective function (2) and at the same time satisfies the condition (9).

In the implementation presented in Ref. [21],  $\rho_{scr}$  was expanded in an auxiliary localized basis set different than the orbital basis. In the present, we expand  $\rho_{scr}$  in products of the basis set functions instead. The motivation for this choice is that as the orbitals are already expanded in finite basis sets with elements  $\chi_k(\mathbf{r})$ , then any density (e.g.  $\rho_t, \rho_u$ ) of the form  $\rho(\mathbf{r}) = \sum_i n_i |\phi_i(\mathbf{r})|^2$ , where  $n_i$  is the occupation number for the orbital  $\phi_i$ , can be written as

$$\rho(\mathbf{r}) = \sum_{kl} D_{kl} \chi_k^*(\mathbf{r}) \chi_l(\mathbf{r}), \quad \text{with } D_{kl} = \sum_i n_i c_k^i c_l^i, \quad (10)$$

where  $c_k^i$  are the orbital expansion coefficients and the matrix  $D$  is the density matrix in the basis set representation.

The procedure we propose in this work is easily incorporated into existing atomic and molecular codes based on a localized basis due to the following advantages: (i) No auxiliary basis for the expansion of  $\rho_{\text{scr}}$  is required. (ii) The usual two electron integrals, available in standard computer codes are necessary for the calculation of the potential matrix elements. On the contrary, by expanding the screening density in an auxiliary basis, as in Ref. [21], additional three-function integrals are also required. (iii) No additional re-expansion of  $\delta\rho$  in any auxiliary basis is required for the update of  $\rho_{\text{scr}}$  in every step. (iv) The Coulomb repulsive potential can be represented exactly in terms of the basis-element products. Thus, the optimization in terms of the total screening density (that includes the Coulomb part) is equivalent to the optimization in terms of the xc part alone.

We now describe the computational procedure to optimize the screening density and hence the repulsive potential,  $u(\mathbf{r})$ . First, we initialize the screening density by specifically defining its corresponding density matrix  $D_{\text{scr}}$ . A reasonable choice is

$$D_{\text{scr}}^{(0)} = \frac{N-1}{N} D_t, \text{ so } \rho_{\text{scr}}^{(0)} = \frac{N-1}{N} \rho_t, \quad (11)$$

where  $D_t$  is the density matrix of the target density  $\rho_t$ , and the superscript (0) denotes initial value, and subsequently ( $i$ ) stands for the iteration number. We note that, in the vast majority of computational implementations of electronic structure methods, the orbitals are expanded in basis sets rather than calculated on a grid and thus electronic densities are traditionally represented by the corresponding matrices of the density. The quantity that we call matrix of the density (or density matrix) represents expansion of the density in a basis. By using orbital products at  $\mathbf{r}, \mathbf{r}'$ , the matrix of the density yields also the expansion of some one-body reduced density matrix in orbital basis products  $\chi_k^*(\mathbf{r}')\chi_l(\mathbf{r})$ , but this 1-RDM is not expected to be close to the non-idempotent 1-RDM of the interacting system (other than sharing the same density). Minimizing the objective function of Eq. (2), through the successive updating of the screening density with density contributions (see Eq.(7)) confirms that the proposed method is a density inversion method.

With this choice, the initial potential is the Coulomb potential that corresponds to the target density, scaled by  $(N-1)/N$ . With the above choice, the value of  $Q_{\text{scr}}$  is fixed during the variation to that dictated by the correct asymptotic behavior for the local potential. Then an iterative procedure is pursued and at each iteration,  $n$ , the following tasks are performed:

- The matrix elements of  $u^{(n)}(\mathbf{r})$  on the basis elements are calculated through the usual two electron integrals:

$$U_{\mu\nu}^{(n)} = \sum_{kl} (D_{\text{scr}}^{(n)})_{kl} [kl|\mu\nu], \quad (12)$$

where  $[kl|\mu\nu]$  is a two electron integral over the

basis functions with indices  $k, l, \mu, \nu$  (chemists' notation).

- The KS Hamiltonian is constructed, by adding the potential matrix,  $U^{(n)}$ , to the constant sum of kinetic and nuclear-repulsion matrices,  $H_{\text{core}}$ , and is diagonalized:

$$[H_{\text{core}} + U^{(n)}] \phi_i^{(n)}(r) = \varepsilon_i \phi_i^{(n)}(r). \quad (13)$$

Using the updated orbitals  $\{\phi_i^{(n)}(r)\}$ , the electronic density  $\rho_u^{(n)}(\mathbf{r})$ , and the corresponding density matrix  $D_u^{(n)}$  are obtained (Eq. (10)).

- Using the Eq. (7), the screening density matrix  $D_{\text{scr}}^{(n+1)}$  is updated:

$$D_{\text{scr}}^{(n+1)} = D_{\text{scr}}^{(n)} - \epsilon [D_t - D_u^{(n)}]. \quad (14)$$

- The convergence is checked using a criterion that we describe below and, in case of convergence, the iteration procedure is terminated.

Our work has similarities, but also important differences compared to the method by Zhao, Morrison and Parr [48, 49] (ZMP). A detailed discussion of this topic by Callow et al. appears in Ref. [21]. In short, in the ZMP method, the total energy functional is minimized under the constraint that the quantity  $U$  is equal to zero; the constraint is enforced with a Lagrange multiplier  $\Lambda$ , in the total energy minimization. The KS equations are solved for finite  $\Lambda$  and then  $\Lambda$  is extrapolated to infinity. In our work,  $U$  (rather than the total energy) is the objective function to be minimized, and its value can differ from zero at the optimal solution. Both methods use the Fermi-Amaldi potential as a convenient initial guess, which sets the initial screening charge equal to  $N-1$ . In our method, the screening density is the variational parameter, and it is optimized in the OEP fashion. Concerning  $\Lambda$ , our work corresponds to  $\Lambda \rightarrow \infty$ , while the iteration step  $\epsilon$  is a small parameter that should not be confused with  $\Lambda$ .

### III. APPLICATION-RESULTS

The iterative procedure described in section II has been implemented in the HIPPO computer code [50] for molecular calculations that is based on gaussian basis set expansion of the molecular orbitals. In that code, DFT functionals are implemented through the LIBXC [51, 52] library while several RDMFT functionals and their minimization are also available. The target densities from CAS-SCF for atomic and molecular systems were obtained through the GAMESS computer code [53, 54].

For most of our study, we employed the Universal gaussian basis set (UGBS) [55], a relatively large set. One advantage of this choice is that this basis set provides

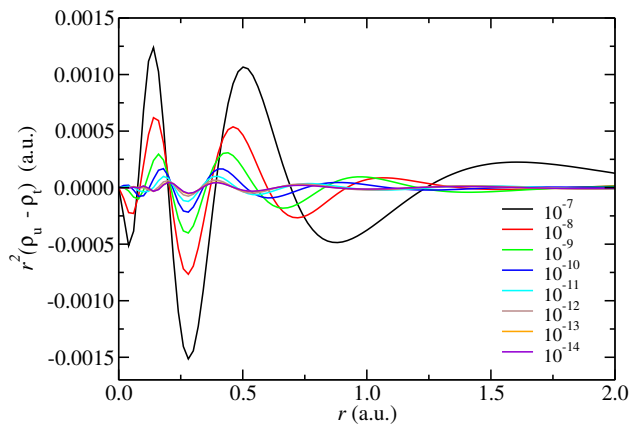


FIG. 1. The quantity  $r^2[\rho_u(\mathbf{r}) - \rho_t(\mathbf{r})]$ , indicating visually the convergence, for several values of the convergence criterion  $c_0$  for Ne for the case of inverting the HF density (UGBS basis set).

one gaussian function for each basis set element, so it allows for a better representation of the densities in both cases of regions of high and low density without imposing additional constraints. We observed that such basis sets lead to smoother potentials.

For the parameter  $\epsilon$ , we found that for a small enough positive constant value, convergence can be achieved. We have chosen  $\epsilon = 0.2$ , but any value of the same order is acceptable. Alternatively, one can devise strategies for updating  $\epsilon$  during iterations. One such strategy, that we found to work, is to scan  $\epsilon$  values keeping the  $D_u^{(n)}$  frozen and pick up the value that lowers mostly the objective function. The choice of constant and small  $\epsilon$  results in slow convergence, thus a significantly larger number of iterations as it limits the correction to the target density in each iteration. However, in this first demonstration, we adopted this choice in order to have better control over convergence.

As far as convergence is concerned, the convergence of several quantities can be considered, like the objective function,  $U_C$ , of Eq. (2) or the absolute difference  $\Delta U_C = |U_C^{(n)} - U_C^{(n-1)}|$  between steps  $n$  and  $n-1$ . Alternatively, for atoms, the quantity  $\alpha = \int r^2 |\rho_u - \rho_t| dr$  is convenient as it suppresses the highly peaked regions near the nuclei. In our calculations and in order to limit the effect of the parameter  $\epsilon$  in the convergence we monitored the quantity

$$c = \frac{\Delta U_C}{\epsilon}, \quad (15)$$

i.e. convergence is assumed when  $c$  becomes smaller than a critical value  $c_0$ . In order to choose the appropriate order of magnitude of  $c_0$  for convergence we plotted the final quantity  $r^2[\rho_u(\mathbf{r}) - \rho_t(\mathbf{r})]$  vs  $r$  for several values of  $c_0$  covering several orders of magnitude ( $10^{-14}$ – $10^{-7}$ ). This analysis for Ne atom is shown in Fig. 1 and as we see  $c_0$  values of the order of  $10^{-11}$  are sufficient for reasonable convergence.

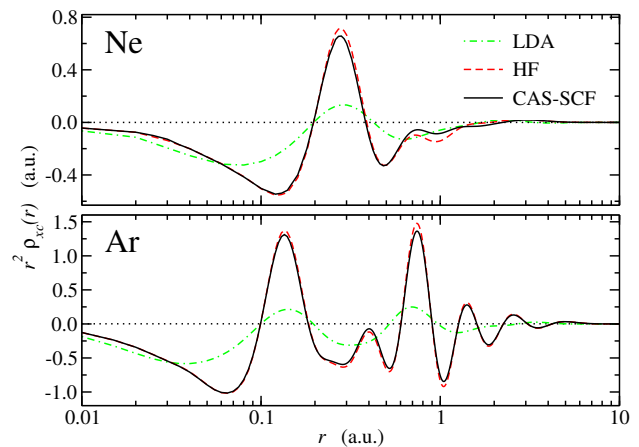


FIG. 2. The xc part of the screening density,  $\rho_{\text{scr}}^{\text{xc}}$ , multiplied by  $r^2$ , for Ne and Ar as a function of the distance  $r$  from the nuclei obtained by inverting the densities that are given by LDA, HF, and CAS-SCF. The xc screening charge is  $Q_{\text{scr}}^{\text{xc}} = -1$  in all cases.

As first applications, we invert densities of 6 atomic and molecular systems that are obtained by KS-LDA and Hartree-Fock (HF). We should note that for KS-LDA the KS potential corresponds (through Poisson's equation) to a screening density that integrates to  $Q_{\text{scr}} = N - a$  with  $a = 0$ . Although for finite basis sets,  $a$  can be different from zero, ( $0 < a < 1$ ), it still differs from the value of 1. Thus, in the case of LDA our constrained inversion leads to a potential that differs from the original LDA potential and satisfies the condition (9). Extensive research on the behavior of the system in the case of LDA, with  $a = 0$ , has been made in Ref. [21]. On the contrary, for HF theory, which is free from self-interactions, the additional condition (9) does not pose a constraint in the optimal inverted potential. That is reflected in Table I, where we present the IPs obtained by inverting LDA and HF densities: Although the IPs from inverting HF densities are close to those obtained by HF eigenvalues, the IPs from inverting the LDA density are highly improved and differ substantially from the values obtained as LDA-KS eigenvalues. We should mention that IPs for LDA with the present approach are close to those obtained by the constrained LDA method of Ref. [39] where the KS potential is replaced by a constrained one satisfying the condition (9).

We now turn our attention to the optimal screening density. In Fig. 2, we show the xc part of the screening densities for Ne and Ar atoms as a function of the radial distance from the nuclei. Clearly, for these noble elements, the screening density from inverting HF density is close to that from CAS-SCF. On the contrary, for LDA, there is a considerable difference, and, although some basic features are also present, the radial dependence is significantly smoothed. Such plots of the xc part of the screening density can provide useful information. As we see in Fig. 2, the xc screening density for Ne is neg-

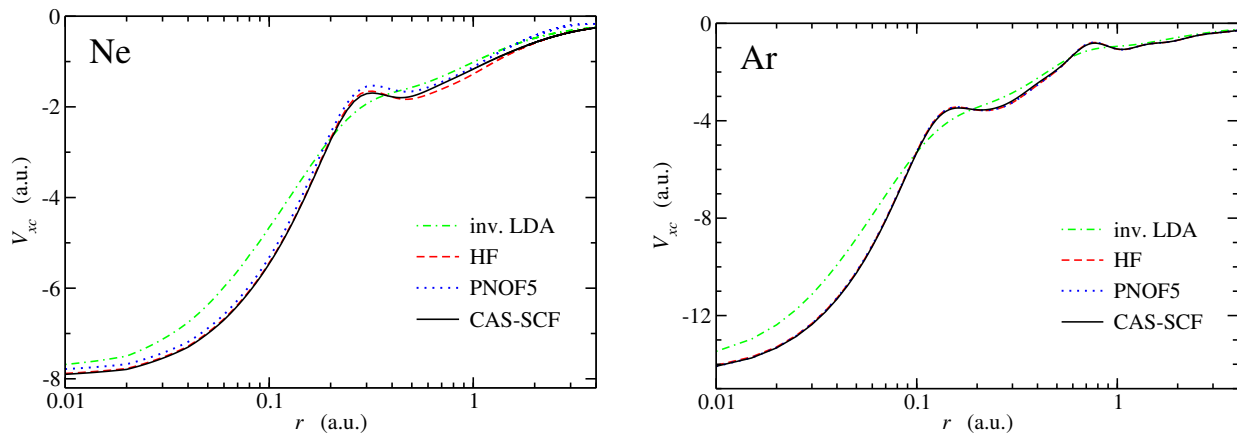


FIG. 3. The xc part of the potentials for Ne (left) and Ar (right) obtained by inverting the densities that are given by LDA, HF, PNOF5 and CAS-SCF approximations. The label “inv. LDA” to distinguish the potential obtained by the (constrained) inversion of the LDA density, satisfying  $Q_{\text{scr}}^{\text{xc}} = -1$ , Eq. (9), from the standard local LDA potential. UGBS basis set was used for all the inversions.

TABLE I. IPs obtained by inverting LDA and HF densities compared with IPs obtained from the KS-LDA and HF eigenvalues

	Inv. LDA	LDA	Inv. HF	HF
He	21.42	15.52	24.98	24.98
Be	8.40	5.60	8.43	8.42
Ne	18.61	13.55	22.83	23.14
Ar	14.24	10.40	16.17	16.08
CO	12.81	9.20	14.51	15.28
CO <sub>2</sub>	12.79	9.35	14.75	14.69

ative for radial distances  $< 0.2$  a.u., leading to a negative xc screening charge accumulation close to the nuclei, followed by a positive peak and a second region of negative density for radial distance  $0.4 \text{ a.u.} < r < 2.15 \text{ a.u.}$  For Ar, the picture is more complicated, however, there are two regions for  $r < 0.1 \text{ a.u.}$  and  $0.2 \text{ a.u.} < r < 0.6 \text{ a.u.}$  where xc screening density is negative and separated by two strong positive peaks. Beyond the second peak, a decaying oscillatory behavior is found. Interestingly, the pronounced peaks of the screening density (one for Ne and two for Ar) correspond to the well known bumps of the xc potential (Fig. 3). For LDA no bumps are present for the xc potential, apparently due to the fact that the peaks in  $\rho_{\text{scr}}^{\text{xc}}$  for LDA are not pronounced enough.

By inverting densities from accurate multi-configurational methods like CAS-SCF, as we show in table II, one can obtain IPs in close agreement with values obtained as energy differences between the positive ion system and the neutral system, i.e.  $\Delta E = E(N-1) - E(N)$ , with  $E(N)$  being the total energy of the system with  $N$  electrons.  $E(N-1)$  and  $E(N)$  arise from two different and independent CAS-SCF calculations. This is evident from the small value of the percent average relative error,  $\delta = 1.4\%$ . The xc part of the potential obtained by inverting densities

	CAS-SCF	
	Inversion	$\Delta E$
He	23.95	23.91
Be	8.17	8.14
Ne	21.60	20.99
Ar	16.13	16.92
H <sub>2</sub> O	12.12	11.95
$\delta$	1.4	

TABLE II. IPs obtained by inverting CAS-SCF densities, using UGBS basis set, compared with values obtained as the differences  $\Delta E$ , of the energy of the neutral systems and their positive ions.  $\delta$  is the percent average relative error  $\delta = (100/N) \sum_i (|x_i - x_i^{(\text{ref})}| / |x_i^{(\text{ref})}|)$ .

from LDA, HF or other methods for Ne and Ar atoms is shown in Figs. 3. Qualitatively the potentials obtained are the same as those in Ref. [21]. Quantitatively minor differences may appear due to the differences between the two methods.

We have also applied the density inversion method to molecular densities obtained by RDMFT calculations. A full RDMFT calculation was performed first and the converged density is obtained as the diagonal of the optimal 1RDM. This density is then inverted to obtain the corresponding local potential. Thus, in this procedure, two sets of orbitals are obtained, the approximate natural orbitals of the full minimization and a set of Kohn-Sham orbitals from the density inversion, which correspond to the single particle KS spectrum. For this application, we used the cc-pVTZ basis sets, while for smaller systems (He, Be, Ne), we also considered cc-pVQZ to investigate the effect of a larger basis set. In table III, we present the IPs obtained for He, Ne, Be atoms using these two different basis sets. As we see in table III, for these atomic systems, the results obtained do not differ much for the two basis sets, there is a good agreement with experimen-

	Müller		BBC3		Power		Exp.
	TZ	QZ	TZ	QZ	TZ	QZ	
He	24.52	24.47	24.15	24.82	24.83	24.82	24.59
Be	7.92	9.61	9.11	9.31	8.67	8.77	9.32
Ne	19.95	19.90	21.15	21.46	20.95	21.15	21.56
$\delta$	7.6	3.8	2.0	0.5	3.6	2.9	

TABLE III. Comparison of IPs of atomic systems obtained by inverting RDMFT densities given by 3 different functionals (Müller, BBC3, and Power) using cc-pVTZ (TZ) and cc-pVQZ (QZ) basis sets with experimental values[56].  $\delta$  is defined in table II.

	BBC3	Power	ML	PNOF5	Exp.
He	24.15	24.83	25.15	24.07	24.59
Be	9.11	8.67	8.61	9.46	9.32
Ne	21.15	20.95	21.56	21.24	21.56
CO	13.12	12.79	13.55	13.77	14.01
N <sub>2</sub>	15.25	15.26	15.56	15.14	15.58
H <sub>2</sub> O	10.76	7.14	12.41	12.57	12.62
CO <sub>2</sub>	13.58	12.49	13.59	13.62	13.77
CH <sub>4</sub>	13.06	13.57	13.60	12.86	12.61
C <sub>2</sub> H <sub>4</sub>	9.51	8.45	9.81	10.45	10.68
$\delta$	5.0	11.4	3.7	1.7	

TABLE IV. Comparison of IPs of molecular systems obtained by inverting RDMFT densities given by different functionals and using cc-pVTZ basis set with experimental values[56].  $\delta$  is defined in table II

tal values, and the error  $\delta$  can be very small. In table IV, we show IPs obtained for a larger set of systems using the cc-pVTZ basis set. Similarly, the overall agreement with experimental values is good, with PNOF5 functional giving the most accurate values ( $\delta = 1.7\%$ ). The xc part of the potentials for Ne and Ar atoms obtained by inverting the densities from PNOF5 are included in Fig. 3.

Inverting the density obtained by a full RDMFT calculation is a way to obtain *a posteriori* a single particle effective system in RDMFT, leading to spectral properties like the ionization potentials. This is a different approach to local-RDMFT[45, 46, 57], a method in which RDMFT functionals are minimized under the constraint that the orbitals come from a single-particle scheme with a local potential. It is thus interesting to compare the IPs obtained by the inversion method with those from local-RDMFT. This comparison is shown in table V, for three different functionals. The results of local-RDMFT in that table are obtained by employing a variant of local-RDMFT where the screening density,  $\rho_{\text{scr}}$  which is the optimization variable is assumed to be given as the square of an amplitude,  $f$ , i.e.  $\rho_{\text{scr}}(r) = f(r)^2$ , and the optimization search is performed in terms of  $f$ . A discussion of this choice and the details of this variant of local-RDMFT will be published elsewhere[58]. As we see in table V, by inverting the density of an RDMFT calculation in the way proposed here, one can obtain single particle prop-

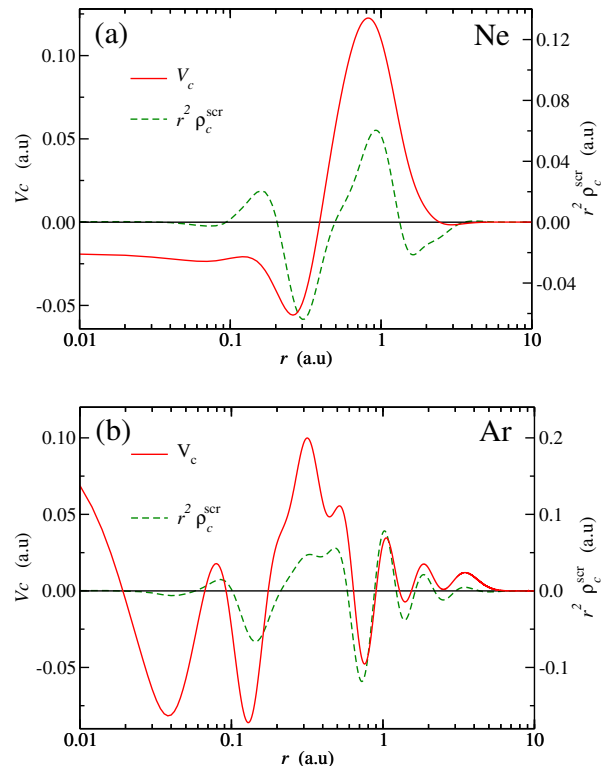


FIG. 4. Correlation potentials and screening densities (multiplied by  $r^2$ ) of Ne (a) and Ar (b), from inverting the CAS-SCF densities to obtain a good approximation of the xc potential (screening density) and subtracting an approximate exchange potential (screening density) taken from inverting the HF density. UGBS basis was used in all required calculations.

erties of similar quality to those of local-RDMFT. It is worth mentioning that for accurate RDMFT functionals, like PNOF5, the quality of the obtained density is such that the IPs from our inversion method are in very good agreement with experiment and comparable to the CAS-SCF results in table II.

The inversion method can be used to obtain correlation potentials, which in the case of exact densities provide a reference for comparison of density functional approximations. To obtain the correlation potential one needs to have a good approximation for the exchange potential to subtract from the xc potential. Here, we used the inverted Hartree-Fock (LFX[36]) potential as an accurate representation of the exact exchange potential and subtracted it from the xc potential obtained from inverting the CAS-SCF density. In Fig. 4, we show the correlation potentials obtained for Ne and Ar atoms. Similarly, the correlation component of the screening density can be obtained as the difference between the CAS-SCF and HF screening densities. In Fig. 4, we also show the correlation screening densities for Ne and Ar atoms, calculated from the data of Fig. 2. The obtained correlation potentials are in good agreement with similar plots of such potentials in the literature [21, 59]. As the correlation potential is a small quantity and more prone to

	Inv. BBC3	Local BBC3	Inv. ML	Local ML	Inv. PNOF5	Local PNOF5	Exp.
He	24.15	24.62	25.16	25.05	24.07	24.35	24.59
Be	9.11	8.93	8.61	8.74	9.46	8.72	9.32
Ne	21.15	22.34	21.78	22.76	21.24	22.58	21.56
CO	13.12	14.57	13.55	13.73	13.77	14.37	14.01
N <sub>2</sub>	15.25	16.44	15.56	16.61	15.14	16.63	15.58
H <sub>2</sub> O	10.76	12.90	12.41	13.39	12.41	13.39	12.62
CO <sub>2</sub>	13.58	14.82	13.59	15.23	13.62	14.86	13.77
CH <sub>4</sub>	13.06	14.10	13.60	14.23	12.86	14.12	12.61
C <sub>2</sub> H <sub>4</sub>	9.51	10.59	9.81	10.92	10.45	10.74	10.68
$\delta$	5.0	4.4	3.7	6.0	1.7	5.3	

TABLE V. Comparison of IPs obtained with the inversion method with those from local-RDMFT for several functional. Experimental results are also included.  $\delta$  is defined in table II

numerical instabilities, the quality of our results in Fig. 4 is proof of the stability of our inversion method.

#### IV. CONCLUSIONS

In conclusion, we presented an effective and simple method that solves the density inversion problem, i.e. finds an optimal potential that corresponds to a prescribed ground-state density. Our method is based on the work of Callow et al[21], i.e. it searches for the optimal constrained potential that corresponds to a given screening charge. Its novelty is that it does not require an additional auxiliary basis set for the expansion of the screening density. Instead, in a natural way, this quantity is expanded in products of the orbital-basis elements. We argue that this is a significant simplification for the implementation of the method in existing computer codes. In order to demonstrate the efficiency of the inversion method, we applied it to various ground state densities of molecular systems obtained by HF, DFT, and CAS-SCF calculations. Also, we applied it to invert densities obtained with RDMFT calculations and we argue that this is a feasible way to introduce a single-particle system in RDMFT. For this purpose, we showed that ionization potentials obtained as energy eigenvalues of the

obtained optimal potentials are in close agreement with experimental ones. Finally, we showed that the inversion method provides an efficient way to yield accurate correlation potentials.

#### AUTHOR CONTRIBUTIONS

S. Bousiadi: conceptualization, funding acquisition, investigation, methodology, software, validation, writing – original draft, writing – review and editing; N. I. Gidopoulos: conceptualization, methodology, supervision, validation, writing – original draft, writing – review and editing; N. N. Lathiotakis: conceptualization, methodology, software, supervision, validation, writing – original draft, writing – review and editing.

#### CONFLICTS OF INTEREST

There are no conflicts to declare.

#### ACKNOWLEDGEMENTS

This work was supported by the Hellenic Foundation for Research and Innovation (HFRI) under the HFRI PhD Fellowship grant (Fellowship Number: 1310).

- 
- [1] W. Kohn and L. J. Sham, *Physical review*, 1965, **140**, A1133.
- [2] P. Hohenberg and W. Kohn, *Physical review*, 1964, **136**, B864.
- [3] I. G. Ryabinkin and V. N. Staroverov, *The Journal of chemical physics*, 2012, **137**, 164113.
- [4] C.-O. Almbladh and A. C. Pedroza, *Physical Review A*, 1984, **29**, 2322.
- [5] R. Van Leeuwen and E. Baerends, *Physical Review A*, 1994, **49**, 2421.
- [6] Q. Wu and W. Yang, *The Journal of chemical physics*, 2003, **118**, 2498–2509.
- [7] A. Görling, *Physical Review A*, 1992, **46**, 3753.
- [8] D. S. Jensen and A. Wasserman, *International Journal of Quantum Chemistry*, 2018, **118**, e25425.
- [9] B. Kanungo, P. M. Zimmerman and V. Gavini, *Nature communications*, 2019, **10**, 1–9.
- [10] K. Peirs, D. Van Neck and M. Waroquier, *Physical Review A*, 2003, **67**, 012505.
- [11] A. Kumar, R. Singh and M. K. Harbola, *Journal of Physics B: Atomic, Molecular and Optical Physics*, 2020, **53**, 165002.
- [12] K. Finzel, P. W. Ayers and P. Bultinck, *Theoretical Chemistry Accounts*, 2018, **137**, 1–6.
- [13] A. A. Kananenka, S. V. Kohut, A. P. Gaiduk, I. G. Ryabinkin and V. N. Staroverov, *The Journal of chemical*

- physics*, 2013, **139**, 074112.
- [14] A. Kumar, R. Singh and M. K. Harbola, *Journal of Physics B: Atomic, Molecular and Optical Physics*, 2019, **52**, 075007.
- [15] I. G. Ryabinkin, S. V. Kohut and V. N. Staroverov, *Physical review letters*, 2015, **115**, 083001.
- [16] R. Cuevas-Saavedra, P. W. Ayers and V. N. Staroverov, *The Journal of chemical physics*, 2015, **143**, 244116.
- [17] E. Ospadov, I. G. Ryabinkin and V. N. Staroverov, *The Journal of chemical physics*, 2017, **146**, 084103.
- [18] T. Naito, D. Ohashi and H. Liang, *Journal of Physics B: Atomic, Molecular and Optical Physics*, 2019, **52**, 245003.
- [19] W. Yang and Q. Wu, *Physical Review Letters*, 2002, **89**, 143002.
- [20] Y. Shi and A. Wasserman, *The Journal of Physical Chemistry Letters*, 2021, **12**, 5308–5318.
- [21] T. J. Callow, N. N. Lathiotakis and N. I. Gidopoulos, *The Journal of chemical physics*, 2020, **152**, 164114.
- [22] A. Müller, *Physics Letters A*, 1984, **105**, 446–452.
- [23] S. Goedecker and C. Umrigar, *Physical review letters*, 1998, **81**, 866.
- [24] M. Buijse and E. Baerends, *Molecular Physics*, 2002, **100**, 401–421.
- [25] G. Csányi, S. Goedecker and T. Arias, *Physical Review A*, 2002, **65**, 032510.
- [26] C. Kollmar, *The Journal of chemical physics*, 2004, **121**, 11581–11586.
- [27] M. Piris, *International journal of quantum chemistry*, 2006, **106**, 1093–1104.
- [28] M. A. Marques and N. Lathiotakis, *Physical Review A*, 2008, **77**, 032509.
- [29] O. Gritsenko, K. Pernal and E. J. Baerends, *The Journal of chemical physics*, 2005, **122**, 204102.
- [30] N. Lathiotakis, S. Sharma, J. Dewhurst, F. G. Eich, M. Marques and E. Gross, *Physical Review A*, 2009, **79**, 040501.
- [31] S. Sharma, J. K. Dewhurst, N. N. Lathiotakis and E. K. Gross, *Physical Review B*, 2008, **78**, 201103.
- [32] M. Piris, X. Lopez, F. Ruipérez, J. Matxain and J. Ugalde, *The Journal of chemical physics*, 2011, **134**, 164102.
- [33] M. Piris and J. M. Ugalde, *International Journal of Quantum Chemistry*, 2014, **114**, 1169–1175.
- [34] M. Piris, *Phys. Rev. Lett.*, 2017, **119**, 063002.
- [35] K. Pernal and K. J. Giesbertz, *Density-Functional Methods for Excited States*, 2015, 125–183.
- [36] T. W. Hollins, S. J. Clark, K. Refson and N. I. Gidopoulos, *Journal of Physics: Condensed Matter*, 2016, **29**, 04LT01.
- [37] S. J. Clark, T. W. Hollins, K. Refson and N. I. Gidopoulos, *Journal of Physics: Condensed Matter*, 2017, **29**, 374002.
- [38] N. I. Gidopoulos, *Physical Review A*, 2011, **83**, 040502.
- [39] N. I. Gidopoulos and N. N. Lathiotakis, *The Journal of chemical physics*, 2012, **136**, 224109.
- [40] A. Görling, *Phys. Rev. Lett.*, 1999, **83**, 5459–5462.
- [41] S. Liu, P. Ayers and R. Parr, *JOURNAL OF CHEMICAL PHYSICS*, 1999, **111**, 6197–6203.
- [42] N. H. March, *Phys. Rev. A*, 2002, **65**, 034501.
- [43] S. V. Kohut and V. N. Staroverov, *The Journal of Chemical Physics*, 2013, **139**, 164117.
- [44] N. I. Gidopoulos and N. N. Lathiotakis, *The Journal of Chemical Physics*, 2012, **136**, 224109.
- [45] N. N. Lathiotakis, N. Helbig, A. Rubio and N. I. Gidopoulos, *Physical Review A*, 2014, **90**, 032511.
- [46] N. N. Lathiotakis, N. Helbig, A. Rubio and N. I. Gidopoulos, *The Journal of Chemical Physics*, 2014, **141**, 164120.
- [47] T. C. Pitts, N. N. Lathiotakis and N. Gidopoulos, *JOURNAL OF CHEMICAL PHYSICS*, 2021, **155**, 224105.
- [48] Q. Zhao, R. C. Morrison and R. G. Parr, *Physical Review A*, 1994, **50**, 2138.
- [49] D. J. Tozer, V. E. Ingamells and N. C. Handy, *The Journal of Chemical Physics*, 1996, **105**, 9200–9213.
- [50] For information, contact NL at lathiot@eie.gr. One- and two-electron integrals for the Cartesian Gaussian basis elements were calculated using the GAMESS code [53, 54].
- [51] M. A. Marques, M. J. Oliveira and T. Burnus, *Computer Physics Communications*, 2012, **183**, 2272–2281.
- [52] S. Lehtola, C. Steigemann, M. J. Oliveira and M. A. Marques, *SoftwareX*, 2018, **7**, 1–5.
- [53] M. W. Schmidt, K. K. Baldridge, J. A. Boatz, S. T. Elbert, M. S. Gordon, J. H. Jensen, S. Koseki, N. Matsunaga, K. A. Nguyen, S. Su, T. L. Windus, M. Dupuis and J. A. Montgomery Jr, *J. Comput. Chem.*, 1993, **14**, 1347–1363.
- [54] M. S. Gordon and M. W. Schmidt, *Theory and Applications of Computational Chemistry*, Elsevier, Amsterdam, 2005, pp. 1167 – 1189.
- [55] B. P. Pritchard, D. Altarawy, B. Didier, T. D. Gibson and T. L. Windus, *Journal of Chemical Information and Modeling*, 2019, **59**, 4814–4820.
- [56] P. Linstorm, *J. Phys. Chem. Ref. Data, Monograph*, 1998, **9**, 1–1951.
- [57] I. Theophilou, N. N. Lathiotakis, N. I. Gidopoulos, A. Rubio and N. Helbig, *The Journal of Chemical Physics*, 2015, **143**, 054106.
- [58] T. Pitts, S. Bousiadi, N. N. Lathiotakis and N. I. Gidopoulos, to be published.
- [59] R. J. Bartlett, *The Journal of chemical physics*, 2019, **151**, 160901.